



Short Communication

Flash sintering as a nucleation phenomenon and a model thereof

Kiran S. Naik^{a,b}, Vincenzo M. Sglavo^a, Rishi Raj^{b,*}^a Department of Industrial Engineering, University of Trento, 38123 Trento, Italy^b Department of Mechanical Engineering, University of Colorado at Boulder, Boulder, CO 80309-0427, USA

Received 24 February 2014; received in revised form 22 April 2014; accepted 24 April 2014

Available online 18 June 2014

Abstract

Isothermal field-assisted sintering of two-phase, 50 vol% 3YSZ-alumina composites exhibit an incubation time for the onset of the flash event. Weaker applied fields and lower temperatures lengthen the incubation period. The effect is highly non-linear. For example at 1300 °C and 150 V cm⁻¹ the flash occurs nearly instantaneously (in 10 s), but extends to 2 h at 1275 °C and 65 V cm⁻¹. This behavior is reminiscent of nucleation and growth phenomena in chemically driven experiments involving phase transformations in the solid state. Here, a model for nucleation under electrical driving forces, based upon the growth of embryos of colossal permittivity is presented. Nucleation is the precursor to the onset of a flash. Therefore it occurs at the furnace temperature. Joule heating is a consequence of nucleation not the cause of it.

© 2014 Elsevier Ltd. All rights reserved.

Keywords: Flash sintering; Incubation time; Nucleation and growth**1. Introduction**

Flash sintering is emerging as a distinct mechanism in field assisted sintering of ceramics. The “flash” is initiated above a threshold applied field at a given temperature, while the extent of densification is controlled by the limit on the current density placed at the power supply.¹ The method has been applied to several oxides,^{2–8} SOFCs^{9,10} as well as to non-oxides.¹¹ The effect can be induced by both DC as well as AC electric fields.¹² Among the various mechanisms proposed in the literature, Joule heating remains of the greatest interest,^{13,14} although the temperatures required for nearly instantaneous sintering are far above what can be reasonably well predicted in this way.

The other suggestion has been to say that a defect avalanche in the form of Frenkel pairs is precipitated which ionize into charge neutral defects and electron–hole pairs. The defects enhance diffusion while the e–h pairs induce high conductivity and photoemission.¹⁵ While, this suggestion does explain why diffusion and conductivity are simultaneously enhanced, a quantitative understanding of how it can happen remains obscure.

Some support for the defect induced mechanism is found in residual effects of the flash on defect concentrations in MgO-doped alumina⁴ and in yttria stabilized zirconia.¹⁶

If indeed flash sintering is instigated by the “nucleation” of defects, then it should be accompanied by an incubation time in experiments carried out at isothermal furnace temperatures. Here we report these results, and show that they are related very non-linearly to the applied field. Tentatively, a model for the nucleation of dipole clusters, of abnormally large permittivity, is developed and analyzed to explain these results. Nucleation is a precursor to the onset of the conduction non-linearity, and, therefore, occurs at the furnace temperature. Joule heating is a result of and therefore is subsequent to nucleation.

2. Experiments

The samples were prepared from commercially available tetragonal zirconia (3 mol% yttria stabilized zirconia – 3YSZ) powder (TZ-3YS-E grade; Tosoh Corp., Shunan, Japan) with a particle size of 600 nm. The high purity α -alumina powder (purity >99.99%), was obtained from Taimicron TMDAR, Taimei Chemical Co., Ltd., Tokyo, Japan, and had a particle size of 100 nm. Two phase composites constituted from equal volume fractions (50/50) of 3YSZ and alumina composite was

* Corresponding author. Tel.: +1 303 492 1029.

E-mail address: rishi.raj@colorado.edu (R. Raj).

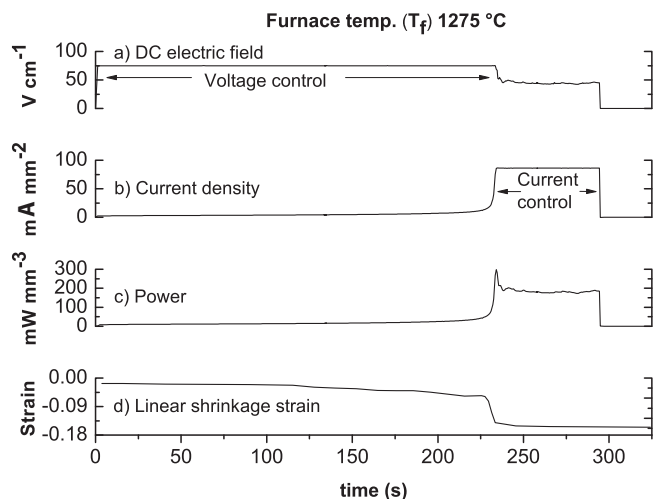


Fig. 1. Isothermal flash sintering versus time curves for (a) DC electric field, (b) current density, (c) power and (d) linear shrinkage strain at 1275 °C for 75 V cm⁻¹.

prepared by following the procedure reported in Ref. 17. Briefly, the 3YSZ and alumina powders were stirred into distilled water, dried and mixed with 3 wt% binder (B-1000, Duramax, Dow Chemical, USA). The powder was then pressed into dog bone shape pellets with gauge length of 21 mm and cross section of 1.8 mm × 3.3 mm.

The experimental setup for the two-electrode field assisted experiments is described in Ref. 17. The samples were hung into a tubular furnace with two platinum wires, which also served as the electrodes. The furnace was first pre-heated at 600 °C for 60 min to burn-off the binder. Thereafter, the furnace was heated at a rate of 10 °C/min up to the required temperature, and then held at this temperature for isothermal experiments. Experiments were performed at four temperatures, 1000 °C, 1200 °C, 1275 °C and 1300 °C. The DC electric field was applied after holding the specimen at temperature for 30 min. The onset of the flash (after an incubation time) was accompanied by a non-linear increase in conductivity, which was controlled by switching the power supply from voltage to current control.¹⁷ Thereafter, the constant current condition was maintained for 60 s, before the power supply was switched off.

The shrinkage in the specimen was measured from photographs taken with a CCD camera at a rate of once every minute before, and at 1 s intervals after the onset of the flash. The specimen temperature, in the flash state, was estimated from a black body radiation model as discussed in detail in Ref. 17. The model requires values of the emissivity which were assumed to lie in the range 0.72–0.9 drawing upon the work on thermal barrier coatings made from yttria stabilized zirconia.

The specimens were cut along the cross section, polished and thermally etched at 1350 °C for 30 min. The micrographs at five different randomly selected places were taken with a SEM (JSM5500, JEOL). The grain size of alumina and zirconia was determined by linear intercept method, with correction factor of 1.56.^{18,19}

A typical specimen response to the applied electric field is given in Fig. 1. In this experiment the furnace temperature

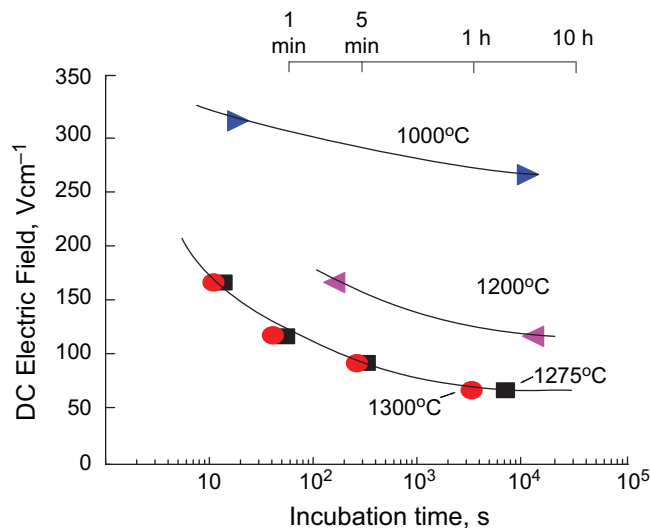


Fig. 2. A semi-log plot of the influence of the electric field on the incubation time at 1000 °C, 1200 °C, 1275 °C and 1300 °C.

was set to 1275 °C, the sample was held at this temperature for 30 min, at which point an electric field of 75 V cm⁻¹ was applied. The time shown in Fig. 1 is from the moment of the application of the field. After an incubation time of 234 s specimen shows the abrupt rise in shrinkage and conductivity. The power supply is then switched to current control with the limit set to 85 mA mm⁻². The flash condition was maintained for 60 s in current control at which point the field was switched off. The power density, equal to the product of the field and the current density, quickly rises to a peak, and then declines as the conductivity of the specimen continues to increase, eventually settling to a steady state, at a field of 50 V cm⁻¹.

The purpose of these experiments was to measure the change in the incubation time for the onset of the flash as a function of the electric field and the furnace temperature. These results are reported in Fig. 2. At a given temperature the incubation time lengthens non-linearly, even on a logarithmic time scale, as the applied field is decreased, suggesting that the electric field serves as the driving force for the nucleation event. As the temperature is lowered, a higher field is required to instill the flash.

The incubation time is related to the growth of an embryo to the critical size, which grows gradually by diffusion. A smaller electric field increases the critical size which lengthens the incubation time. On the other hand a lower temperature requires more time because diffusion is slower.

The microstructures obtained in these experiments were the same as obtained in constant heating rate experiments as described in Ref. 17. The size of alumina and zirconia grains was measured for experiments carried out at furnace temperature of 1275 °C under different levels of applied field. A typical microstructure taken from 100 V cm⁻¹ is shown in Fig. 3. The grain sizes for alumina and zirconia grains at 50 V cm⁻¹, were 693 ± 69 nm, and 684 ± 59 nm. At 73 V cm⁻¹ they were 671 ± 62 nm and 612 ± 10 nm respectively. At 100 V cm⁻¹, 758 ± 118 and 645 ± 40 nm, and at 150 V cm⁻¹, 727 ± 151 and 675 ± 68 nm respectively for alumina and zirconia grains. The specimen temperatures estimated from black body

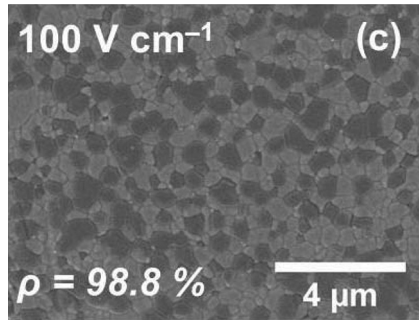


Fig. 3. Micrograph of the grain size obtained from isothermal flash sintering at 1275 °C.

radiation model, using emissivity values in the range 0.73 to 0.92, were 1389–1415 °C, 1394–1421 °C, 1421–1453 °C and 1424–1458 °C at fields of 50, 75, 100 and 150 V cm⁻¹. The densities of these specimens, given at increasing electrical fields were 94.4%, 97.1%, 98.8% and 98%, respectively.

3. A model for nucleation

In isothermal furnace temperature experiments, the flash phenomenon occurs in three stages. The first is the onset of the non-linear conductivity at the applied field. This is the nucleation event, which occurs at the furnace temperature, and embodies an incubation time. The non-linear rise in conductivity is controlled by switching the power supply to current control; this is the second stage. The third stage is the quasi-steady state that is established under current control. Joule heating begins in Stage II and continues in Stage III. Thus flash sintering has two unusual features: (i) the nucleation of the non-linear event, and (ii) and the rapid rate of sintering in the highly conducting state of Stages II and III. Much of the community's (and our) focus has been on the high sintering rates in these later stages, where Joule heating does indeed occur and whose overall role in the process remains controversial. However, the peculiar nucleation of the non-linear transition from insulating to conducting state, which occurs at the furnace temperature, has so far been often overlooked. This paper is concerned with this nucleation event, which precedes Joule heating. It occurs at furnace temperature.

Thermal ionization of interstitials and vacancies above a critical electric field, as analyzed in the Poole–Frenkel model,^{20,21} could also explain the onset of insulator to conducting transition. However, substitution of numbers shows that the fields required for Poole–Frenkel would have to be several orders of magnitude greater than employed in the flash experiments. Furthermore the Poole–Frenkel mechanism does not entail an incubation time.

That the incubation time for nucleation varies highly non-linearly with driving force is well known in solid-state phase transformations. The phenomenon has been discussed under the title of transient nucleation in the early work of Turnbull.^{22,23} The embryo grows slowly gathering the atoms of a precipitating species in the solid-solution, which competes with the dissolution of the embryo, until it reaches a supercritical size.

The following analysis is based upon these early concepts. We hypothesize that an embryo of high dielectric constant is

formed under the influence of the electric field. The high dielectric constant is assumed, rather elementarily, to arise from the aggregation of aligned dipoles made of the vacancy-interstitial Frenkel pairs. It is relevant that very high relative dielectric constants, referred to as colossal permittivity have been discussed in barium titanate when the grain size is of nanoscale dimensions.²⁴ Values as high as 10⁶ have been reported.²⁵ In at least one instance permittivity of 3 × 10⁵ in large grained (several hundred nm) barium titanate prepared by microwave sintering has been reported.²⁶ In the nucleation phenomenon we are concerned with embryos just a few nm in diameter, much smaller than the grain size where these colossal permittivities have been measured. Phenomenologically it appears that a smaller dimension leads to a higher permittivity. Therefore, the assumption that the embryos have permittivity at least in the 10⁵–10⁶ range is justifiable. We expect that this point will remain of interest in future studies of this nucleation phenomenon.

The driving force for nucleation arises from the polarization energy of this aggregate of a high dielectric constant. This energy, per unit volume, ΔG_V , is given by

$$\Delta G_V = \frac{1}{2} \varepsilon_o \varepsilon_E E_j^2 \quad (1)$$

where ε_o is the permittivity of vacuum, ε_E is the dielectric constant of the embryo, and E_j is the applied electric field.

The growth of the embryo is opposed by the energy of the interface it forms with the parent lattice, which we call γ_E . The total free energy of the embryo, relative to the zero field state, is then given by

$$\Delta G = -4\pi r^3 \Delta G_V + 4\pi r^2 \gamma_E \quad (2)$$

Eq. (2) reaches a maximum, the critical state, when

$$\left(\frac{\partial \Delta G}{\partial r} = 0 \right)_{r=r^*} \quad (3)$$

Substituting Eq. (2) into (3), and then putting back the value for r^* so obtained into Eq. (2) obtains the following relationships

$$r^* = \frac{2\gamma_E}{\Delta G_V} \quad (4)$$

and

$$\Delta G^* = \frac{1}{2} \left(\frac{4\pi}{3} r^{*3} \right) \Delta G_V \quad (5)$$

where ΔG^* is the free energy barrier expressed at the critical state of the embryo. Substituting Eq. (1) into (4), gives

$$r^* = \frac{4\gamma_E}{\varepsilon_o \varepsilon_E E_j^2} \quad (6)$$

The incubation time, which is the time required to grow the embryo slowly uphill toward a critical size, increases highly non-linearly with the number of atom-species in the critical nucleus.²³ It also depends on the mobility of the species in the region surrounding the embryo. Typically a critical size of a few tens of nanometers is realizable within the laboratory time scale at elevated temperatures, where solid state diffusion occurs at a

Table 1
Estimates of the critical embryo radius from Eq. (6).

E_j , V cm ⁻¹	ε_E	γ_E , mJ m ⁻²	r^* , nm
1000	10 ⁶	1	45
3000	10 ⁶	1	5
1000	10 ⁶	10	450
3000	10 ⁶	10	50

measurable rate. Thus the size of the critical nucleus becomes a measure of the incubation time.

We consider the size of r^* estimated from Eq. (6). Although the local field within the material may be enhanced by inhomogeneities, to a first approximation we set E_j equal to the applied field, keeping in mind that this would be the lower bound for the driving force for nucleation. The interfacial energy γ_E is likely to be very low since the embryo will be coherent with the parent matrix, its magnitude arising from the energy of the dipoles at the surface relative to those within the embryo. There is an equivalence with the energy of the domain walls in ferroelectric crystals formed between regions of opposite (or orthogonal) polarizations. These walls can be several atom layers wide. Their energy is calculated to be 1–10 mJ m⁻².²⁷ In the present case the energy is likely to be considerably lower since the dipoles exist only within the embryo, and the interface can be expected to be sharp. We shall assume that $\gamma_E = 1$ mJ m⁻², recognizing well that future discussions of the nucleation mechanism are likely to center on the atomic and electronic structure and its relationship to energy and kinetics of the embryo–matrix interface.²⁸

It remains to consider a value for the dielectric constant. With a high density of charged dipoles it is expected to be very high, and we assume it to lie in the range $\varepsilon_E = 10^5 - 10^6$, as discussed above.^{24–26} The physical constant $\varepsilon_0 = 8.85 \times 10^{-12}$ Fm⁻¹. The estimates of r^* calculated in this manner are given in Table 1. The values for the embryo size for the assumed values of the interfacial energy and dielectric constant are within the bounds of experimental results.

A major uncertainty in the analysis is the assumption of the local field at the embryo being equal to the applied field. In fact inhomogeneities in the microstructure, such as grain boundaries and dislocations can intensify the local field. Since the embryo size varies inversely as the square of the field, a high value, locally, can substantially reduce the barrier to nucleation.

Another way of analyzing the nucleation phenomenon is to calculate the probability of nucleation, p_E , given by

$$p_E = \exp\left(-\frac{\Delta G^*}{k_B T}\right) \quad (7)$$

Substituting from Eq. (5) leads to the plots shown in Fig. 4 (for $T = 1000$ K, and $\varepsilon_E = 10^6$). The plots show the highly nonlinear increase in p_E with E_j , for three values of γ_E . The threshold value for the nucleating field can be estimated from the asymptotes to the curves. The steepness of the curves, especially in view of the logarithmic scale for p_E is characteristic of a nucleation phenomenon.

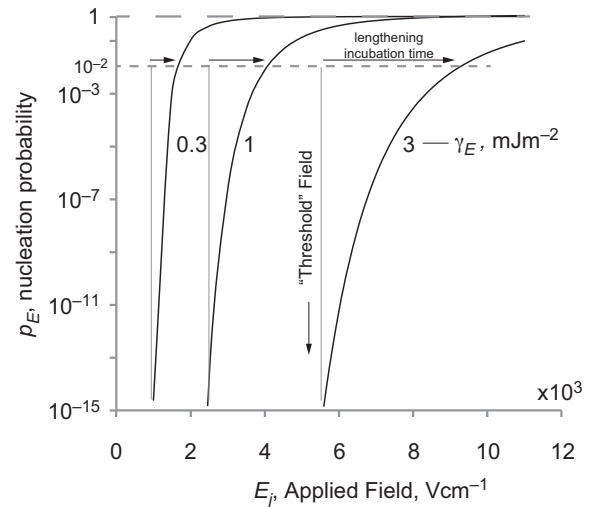


Fig. 4. Plots for the probability of nucleation as a function of the interfacial energy. $T = 1000$ K, and $\varepsilon_E = 10^6$.

4. Summary

The phenomenon of flash sintering has the characteristics of nucleation and growth. The nucleation event is the abrupt transition from insulating to conducting state in the ceramic. It is instigated when a critical field is applied while the specimen is held at a constant temperature, equal to that of the furnace. The nucleation event embodies an incubation time that lengthens from a few seconds to several thousand seconds as the applied field is reduced. This relationship of the incubation time to the applied field confirms that the electrical field is the driving force for the nucleation mechanism.

Nucleation phenomena are defined by a volumetric driving force which favors the event, and the interfacial energy which opposes it. The surface to volume ratio of the embryo determines the probability of nucleation and the incubation time to reach a nucleus of the critical size. The analysis presented above assumes that the polarization energy of the embryo, under the applied electric field, is the driving force for nucleation.

If the hypothesis is correct, then the issue of the interface between the embryo and the matrix gains great scientific significance. The interface is not only important in its energy, but also in how it produces an avalanche of defects, once a supercritical state is reached. These questions of interfacial polarization and generation of electrons and holes is being studied in ab-initio calculations of heterointerfaces.²⁷ There, however, the creation of the “electron gas” is postulated to remain localized near the interface. The new question in the context of flash sintering is that the electron gas spreads throughout the specimen inducing the entire specimen to become electronically conducting.

In addition to the energy and the atomic structure of the interface, the dielectric constant of the embryo, which determines the polarization energy, is a critical parameter in the nucleation model. We postulate the embryo to consist of aligned dipoles, much like in ferroelectric ceramics. Values of permittivity in the 10^5 – 10^6 range yield plausible values for the critical size of the embryos.

Both these parameters, interface structure and polarization of the embryos, will remain of fundamental interest in further studies of why there is the abrupt transition from the insulating to the conducting state. Why this transition is followed by ultrahigh rates of self-diffusion is a further mystery in flash sintering.

It is worthwhile to keep in mind that nucleation occurs at the furnace temperature. Joule heating is a consequence of the nucleation of the flash event. It cannot be its cause.

Acknowledgements

The author would like to express great appreciation to Dr. John Francis, Mr. Shikhar Jha for their help and useful suggestions during the period of this study. The work was supported at the University of Colorado by the Basic Energy Sciences Division of the Department of Energy under Grant No. DE-FG02-07ER46403. KSN thanks the University of Trento, Italy for supporting his visit to Colorado.

References

- Francis JSC, Raj R. Influence of the field and the current limit on flash sintering at isothermal furnace temperatures. *J Am Ceram Soc* 2013;**96**:2754–8.
- Cologna M, Rashkova B, Raj R. Flash sintering of nanograin zirconia in <5 s at 850 °C. *J Am Ceram Soc* 2010;**93**:3556–9.
- Cologna M, Prette ALG, Raj R. Flash-sintering of cubic yttria-stabilized zirconia at 750 °C for possible use in SOFC manufacturing. *J Am Ceram Soc* 2011;**94**:316–9.
- Cologna M, Francis JSC, Raj R. Field assisted and flash sintering of alumina and its relationship to conductivity and MgO-doping. *J Eur Ceram Soc* 2011;**31**:2827–37.
- Karakuscu A, Cologna M, Yarotski D, Won J, Francis JSC, Raj R, et al. Defect structure of flash-sintered strontium titanate. *J Am Ceram Soc* 2012;**95**:2531–6.
- Jha S, Raj R. The effect of electric field on sintering and electrical conductivity of titania. *J Am Ceram Soc* 2013;**8**:1–8.
- Muccillo R, Muccillo ENS. Electric field-assisted flash sintering of tin dioxide. *J Eur Ceram Soc* 2014;**34**:915–23.
- Yoshida H, Sakka Y, Yamamoto T, Lebrun J-M, Raj R. Densification behaviour and microstructural development in undoped yttria prepared by flash-sintering. *J Eur Ceram Soc* 2014;**34**:991–1000.
- Downs Ja, Sglavo VM. Electric field assisted sintering of cubic zirconia at 390 °C. *J Am Ceram Soc* 2013;**96**:1342–4.
- Francis JSC, Cologna M, Montinaro D, Raj R. Flash sintering of anode-electrolyte multilayers for SOFC applications. *J Am Ceram Soc* 2013;**96**:1352–4.
- Zapata-Solvas E, Bonilla S, Wilshaw PR, Todd RI. Preliminary investigation of flash sintering of SiC. *J Eur Ceram Soc* 2013;**33**:2811–6.
- Steil MC, Marinha D, Aman Y, Gomes JRC, Kleitz M. From conventional ac flash-sintering of YSZ to hyper-flash and double flash. *J Eur Ceram Soc* 2013;**33**:2093–101.
- Raj R. Joule heating during flash-sintering. *J Eur Ceram Soc* 2012;**32**:2293–301.
- Narayan J. A new mechanism for field-assisted processing and flash sintering of materials. *Scr Mater* 2013;**69**:107–11.
- Raj R, Cologna M, Francis JS. Influence of externally imposed and internally generated electrical fields on grain growth, diffusional creep, sintering and related phenomena in ceramics. *J Am Ceram Soc* 2011;**94**:1941–65.
- M'Peko J-C, Francis JSC, Rishi Raj. Impedance Spectroscopy and Dielectric Properties of Flash Versus Conventionally Sintered Yttria-Doped Zirconia Electroceramics Viewed at the Microstructural Level. *J Am Ceram Soc* 2013;**96**(12):3760–7.
- Naik, Kiran S, Vincenzo M, Sglavo, Rishi Raj. Field assisted sintering of ceramic constituted by alumina and yttria stabilized zirconia. *J Eur Ceram Soc* 2014;**34**(10):2435–42.
- Mendelson M. Average grain size in polycrystalline ceramics. *J Am Ceram Soc* 1969;**52**:443–6.
- Wurst J, Nelson J. Lineal intercept technique for measuring grain size in two phase polycrystalline ceramics. *J Am Ceram Soc* 1972;**46**:109.
- Simmons JG. Poole–Frenkel effect and Schottky effect in metal–insulator–metal systems. *Phys Rev* 1967;**155**:657.
- Frenkel J. On pre-breakdown phenomena in insulators and electronic semiconductors. *Phys Rev* 1938;**54**(8):647.
- Fisher JC, Hollomon JH, Turnbull D. Nucleation. *J Appl Phys* 2004;**19**(8):775–84.
- Turnbull D. Transient nucleation. *Met Technol* 1948:15.
- Guillemet Fritsch S, Valdez Nava Z, Tenailleau C, Lebey T, Durand B, Chane Ching JY. Colossal permittivity in ultrafine grain size BaTiO_{3-x} and Ba_{0.95}La_{0.05}TiO_{3-x} materials. *Adv Mater* 2008;**20**(3):551–5.
- Hu W, Liu Y, Withers RL, Frankcombe TJ, Norén L, Snashall A, et al. Electron-pinned defect-dipoles for high-performance colossal permittivity materials. *Nat Mater* 2013;**12**(9):821–6.
- (a) Han H, Ghosh D, Jones JL, Nino JC. Colossal permittivity in microwave sintered barium titanate and effect of annealing on dielectric properties. *J Am Ceram Soc* 2013;**96**(2):485–90;
(b) Arlt G, Hennings D. Dielectric properties of fine grained barium titanate ceramics. *J Appl Phys* 1985;**58**(4):1619–25.
- Zunger A, University of Colorado at Boulder, private communication.